

LETTER | JULY 06 2022

## Mechanism for sequestering magnetic energy at large scales in shear-flow turbulence **FREE**

B. Tripathi ; A. E. Fraser ; P. W. Terry ; E. G. Zweibel ; M. J. Pueschel 



*Physics of Plasmas* 29, 070701 (2022)

<https://doi.org/10.1063/5.0096886>

 CHORUS



View  
Online



Export  
Citation

CrossMark

### Articles You May Be Interested In

Sequestering in models of F-term uplifting

*AIP Conference Proceedings* (November 2008)

Constraints of the  $B \mu / \mu$  Solution in the Gauge Mediation via the Conformal Sequestering

*AIP Conference Proceedings* (November 2008)

Probing the Sequestering of Carbon Nanotubes in the PS Domains of SIS Block Copolymer Matrix using Electrostatic Force Microscopy

*AIP Conference Proceedings* (June 2010)

# Mechanism for sequestering magnetic energy at large scales in shear-flow turbulence

Cite as: Phys. Plasmas **29**, 070701 (2022); doi: [10.1063/5.0096886](https://doi.org/10.1063/5.0096886)

Submitted: 22 April 2022 · Accepted: 13 June 2022 ·

Published Online: 6 July 2022



View Online



Export Citation



CrossMark

B. Tripathi,<sup>1,a)</sup>  A. E. Fraser,<sup>2,b)</sup>  P. W. Terry,<sup>1,c)</sup>  E. G. Zweibel,<sup>1,d)</sup>  and M. J. Pueschel<sup>3,4</sup> 

## AFFILIATIONS

<sup>1</sup>University of Wisconsin-Madison, Madison, Wisconsin 53706, USA

<sup>2</sup>University of California, Santa Cruz, California 95064, USA

<sup>3</sup>Dutch Institute for Fundamental Energy Research, 5612 AJ Eindhoven, The Netherlands

<sup>4</sup>Eindhoven University of Technology, 5600 MB Eindhoven, The Netherlands

<sup>a)</sup> Author to whom correspondence should be addressed: [bttripathi@wisc.edu](mailto:bttripathi@wisc.edu)

<sup>b)</sup> Electronic mail: [adfraser@ucsc.edu](mailto:adfraser@ucsc.edu)

<sup>c)</sup> Electronic mail: [pwterry@wisc.edu](mailto:pwterry@wisc.edu)

<sup>d)</sup> Electronic mail: [zweibel@astro.wisc.edu](mailto:zweibel@astro.wisc.edu)

## ABSTRACT

Straining of magnetic fields by large-scale shear flow, which is generally assumed to lead to intensification and generation of small scales, is reexamined in light of the persistent observation of large-scale magnetic fields in astrophysics. It is shown that, in magnetohydrodynamic turbulence, unstable shear flows have the unexpected effect of sequestering magnetic energy at large scales due to counteracting straining motion of nonlinearly excited large-scale stable eigenmodes. This effect is quantified via dissipation rates, energy transfer rates, and visualizations of magnetic field evolution by artificially removing the stable modes. These analyses show that predictions based upon physics of the linear instability alone miss substantial dynamics, including those of magnetic fluctuations.

Published under an exclusive license by AIP Publishing. <https://doi.org/10.1063/5.0096886>

Turbulence is a fundamentally multiscale process in which nonlinear dynamical motions carry energy across scales.<sup>1,2</sup> One of the most robust and extensively studied mechanisms for cross-scale energy transfer is straining by shear flow,<sup>2,3</sup> long recognized for its role in cascades to small scale.<sup>4</sup> This process is especially active in magnetohydrodynamic (MHD) turbulence.<sup>5</sup> The stretching, squeezing, and folding of magnetic field lines by shear flow are readily discernible in visualizations and lead to, for example, the enhancement of small-scale resistive dissipation and the intensification of magnetic energy at small scales beyond the viscous cutoff in turbulence with the magnetic Prandtl number greater than unity.<sup>5,6</sup> The ubiquity of turbulence and turbulent straining is at odds with the well-established observations of magnetic fields at large scales in the universe (stellar, galactic, and beyond)<sup>7,8</sup> and part of a conundrum as to how magnetic fields exist at such large scales.<sup>9–11</sup>

In this Letter, we report the first observations that magnetic energy is, to a considerable degree, counterintuitively sequestered at large scales in straining by a paradigmatic turbulent shear flow. The result applies to a Kelvin–Helmholtz (KH)-unstable flow maintained by an external force with a uniform magnetic field that is initially

flow-aligned and, therefore, optimally configured to promote small-scale generation.

The process that counteracts the small scale generation of magnetic energy, which is quantified in this Letter, can be traced to the nonlinear excitation of large-scale stable linear eigenmodes.<sup>12</sup> The dispersion relation that is associated with the shear-flow instability present in this study has a stable (damped) root, which acts to return energy and momentum to the mean profile and which is excited to a high level by the nonlinearity.<sup>13,14</sup> The nonlinear excitation of stable modes and its effect on turbulence levels and transport have been studied previously, particularly in the context of fusion-relevant gyroradius-scale turbulence.<sup>12,15–23</sup> Recent studies have shown that stable modes are also excited in macroscopic shear-flow driven turbulence and transiently affect momentum transport.<sup>13,14</sup> However, critical features of counteracting straining motion of the stable modes, essential for large-scale sequestering of magnetic energy, have only come to light in the study described here.

Moreover, stable-mode effects have been linked to small-scale dissipation,<sup>20</sup> suggesting that they affect turbulence only if there is an increase in entropy. However, we show here that the reversible process

by which stable modes return energy to the mean flow, in opposition to extraction by the instability, is quite effective at blunting the energy cascade to small scales. Stable modes have been connected to the shear-layer contraction (i.e., build-up of mean flow)<sup>14</sup> but only as a transient process. Here, we demonstrate that for a driven flow profile, the return of fluctuation energy to the mean profile occurs continuously at a rate that nearly matches the rate at which unstable modes attempt to flatten the flow profile.

The principal result of this Letter is that, in driven shear-flow MHD turbulence, the nonlinearly excited large-scale stable eigenmodes efficiently strain the magnetic fields in a way that counteracts the effect of unstable modes and, thus, greatly weakens the magnetic energy cascade to small scales.

We study an incompressible, two-dimensional (2D) system with the initial fluid velocity given as  $\mathbf{v}(x, z, t = 0) = U_{\text{ref}}(z)\hat{\mathbf{x}} = U_0 \tanh(z/a)\hat{\mathbf{x}}$  and an initially uniform flow-aligned magnetic field as  $\mathbf{B}(x, z, t = 0) = B_0\hat{\mathbf{x}}$ . The parameters  $a$ ,  $U_0$ , and  $B_0$  represent the half-width of the flow-shear, the maximum fluid velocity, and the magnetic field strength, respectively, which are used to non-dimensionalize all the variables henceforth. Consequently, time and energy (per unit mass) have units of  $a/U_0$  and  $U_0^2$ . We describe the flow and the magnetic field by a stream function  $\phi$  and a flux function  $\psi$ , where  $\mathbf{v} = \hat{\mathbf{y}} \times \nabla\phi$  and  $\mathbf{B} = \hat{\mathbf{y}} \times \nabla\psi$ . We study their evolution using the momentum and induction equations of the standard MHD (see Ref. 24 and the supplementary material)

$$\partial_t \nabla^2 \phi = -\{\nabla^2 \phi, \phi\} + M_A^{-2} \{\nabla^2 \psi, \psi\} + \text{Re}^{-1} \nabla^4 \phi + \partial_z f(k_x = 0, z, t), \quad (1a)$$

$$\partial_t \psi = \{\phi, \psi\} + \text{Rm}^{-1} \nabla^2 \psi, \quad (1b)$$

where  $\nabla^2 \phi$  and  $\nabla^2 \psi$  are the vorticity and the current density, respectively; the Poisson bracket is  $\{P, Q\} \equiv \partial_x P \cdot \partial_z Q - \partial_x Q \cdot \partial_z P$ ; the Alfvénic Mach number is  $M_A \propto U_0/B_0$ ; the fluid and magnetic Reynolds numbers are defined as  $\text{Re} = U_0 a/\nu$  and  $\text{Rm} = U_0 a/\eta$ . In this study, we take  $\text{Re} = 500$ . Except for simulations where  $\text{Rm} = 50$  and  $\text{Rm} = 5000$  (which will be stated explicitly), all others have  $\text{Rm} = 500$ . In Eq. (1a),  $f$  represents a body force that continuously regenerates the mean-flow shear. The expression  $k_x = 0$  in it indicates that the force acts only on the ( $x$ -averaged) mean flow, where  $k_x$  is the Fourier wavenumber. The forcing, thus, prevents gradual flattening of

the mean flow as the instability extracts energy from it. A similar process occurs in astrophysical flows, where forces like gravitation replenish continually the shear profile, e.g., shear layers in accretion disks, stars, and planetary atmospheres. We represent this force by a Krook-like operator,<sup>25–27</sup> sometimes referred to as a profile relaxation term,<sup>28</sup>

$$f = D_{\text{Krook}} [U_{\text{ref}}(z) - \langle U(x, z, t) \rangle_x] + F_0, \quad (2)$$

where  $D_{\text{Krook}}$  represents the rate at which the mean flow is forced toward the reference flow profile. We choose  $D_{\text{Krook}} = 2$ . Detailed analyses of a complete scan of different parameters will be reported elsewhere. The force  $F_0$  balances the viscous diffusion of the mean shear layer,  $\text{Re}^{-1} \nabla^2 U_{\text{ref}}(z) + F_0 = 0$ , in Eq. (1a), to ensure an initial equilibrium state.

We add small-amplitude perturbations to the flow and the magnetic field (see Ref. 14 and the supplementary material) and perform time-integration of the above set of equations using the pseudospectral code Dedalus<sup>29</sup> for long times ( $t > 1000$ ; the e-folding growth time of the instability is  $\approx 6$ ). Apart from the simulation of  $\text{Pm} = 10$  that uses a spectral resolution of 4096 Fourier (Chebyshev) modes along the  $x$ -( $z$ -) axis for the box size of  $(L_x, L_z) = (6\pi, 8\pi)$ , all other simulations are performed at  $2048 \times 2048$  spectral resolution for the box size of  $(L_x, L_z) = (10\pi, 20\pi)$ , while convergence checks utilize resolutions as high as  $8192 \times 8192$  with no substantial impact on dissipation rates and spectral energy densities. (All simulations additionally use a 3/2 dealiasing rule.<sup>29</sup>)

We also perform a corresponding eigenvalue calculation of the non-dissipative equations, derived from Eqs. (1a) and (1b), by linearizing about the initial flow and magnetic field profiles.<sup>14</sup> *A priori*, one does not know whether such an eigenmode basis is useful to understand turbulent features. Nevertheless, since the eigenmodes of this linear operator form a complete (albeit non-orthogonal) basis,<sup>30,31</sup> we can expand the time-evolving state space of nonlinear simulations in this basis after determining amplitude  $\beta_j(k_x, t)$  of each eigenmode  $j$  at each  $k_x$  as a function of time,  $\tilde{\chi}_{\text{turbulent}}(x, z, t) = \sum_{k_x; k_x \neq 0} e^{ik_x x} [\sum_j \beta_j(k_x, t) \chi_j(k_x, z)]$ , where  $\tilde{\chi}_{\text{turbulent}} = (\tilde{\phi}_{\text{turbulent}}, \tilde{\psi}_{\text{turbulent}})$  captures the turbulent state space and  $\chi_j$  is the  $j$ th eigenmode.<sup>14,32–34</sup> This procedure is illustrated in Fig. 1(a), where the eigenmodes of the flow fluctuations are shown. (The magnetic fluctuations have eigenmodes<sup>14</sup> and parity<sup>37,38</sup> related to those of the flow fluctuations.)

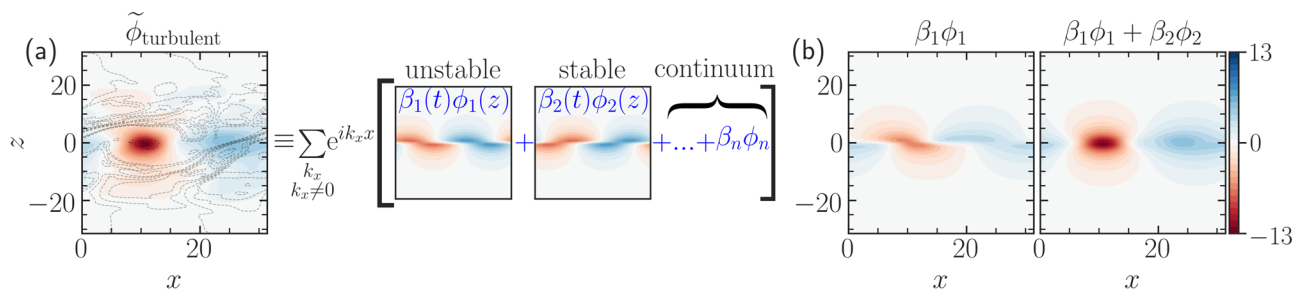


**FIG. 1.** (a) Eigenmode decomposition of a characteristic snapshot of the turbulent flow, represented by the solid- and colored-contour lines of the stream function  $\phi_{\text{turbulent}}$  at time  $t = 625$  with  $M_A = 10$ . The decomposition is based on a complete set: unstable, stable, and continuum eigenmodes. The eigenmodes plotted are for the flow fluctuations at the first Fourier wavenumber. The black dashed-contour lines overplotted on the first image show the turbulent magnetic flux function  $\psi_{\text{turbulent}}$ , whose distortion near the center of the eddy,  $(x, z) \approx (10, 0)$ , is significantly impeded. (b) Reconstruction of the turbulent flow: (left) sum of unstable eigenmodes at each Kelvin–Helmholtz-unstable wavenumber; (right) improvement by adding their conjugate stable eigenmodes. Compare these with full  $\phi_{\text{turbulent}}$  in (a). The difference between the plots (a) and (b) is shown in the supplementary material. All panels here share the same colorbar.

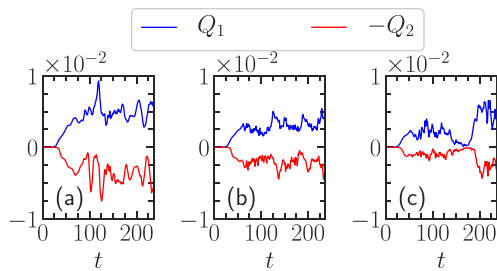


**FIG. 2.** Time trace of  $Q_1$  (blue) vs  $-Q_2$  (red) for (a)  $Pm = 0.1, Rm = 50$ ; (b)  $Pm = 1, Rm = 500$ ; (c)  $Pm = 10, Rm = 5000$ . Compare the lower (red) with upper (blue) curves within each subplot. To illustrate similar variation of  $Q_1$  and  $Q_2$  and to make the variations maximally visible, we plot  $-Q_2$ , which physically refers to the energy transfer rate from the fluctuations to the mean profiles. Computationally demanding simulation for (c) was stopped at  $t = 237$ . All simulations use  $M_A = 10$ . Nonlinear phase begins at  $t \sim 30$ . Energy available for cascading to small scales is significantly impeded by stable modes in all cases.

At each wavenumber  $k_x$ , linearly unstable to perturbations (i.e.,  $0 < k_x < 1$  for the present shear-flow instability), there is an unstable eigenmode  $\phi_1$  and its conjugate stable eigenmode  $\phi_2$  with eigenvalues complex conjugate to each other.<sup>13,39</sup> All the remaining eigenmodes have purely real eigenfrequencies,<sup>32</sup> belong to the continuum<sup>40</sup> and have narrow structures along the  $z$ -axis.

Tracking the time evolution of each eigenmode amplitude  $\beta_j(k_x, t)$  in the nonlinear simulations, the initially exponentially decaying mode has been found to be nonlinearly excited to almost the same level as the unstable mode.<sup>14</sup> The driving mechanism for this excitation is, at early times, the nonlinear interaction between the unstable modes, see, e.g., Refs. 14, 22, and 23. In the fully nonlinear phase, however, all modes that have large energy interact dominantly.

For a given KH-unstable wavenumber, it is found, in Fig. 1(b), that a combination of two eigenmodes from the above basis reconstructs the large-scale turbulent flow at that wavenumber. Figure 1(b) shows a reconstruction of the turbulent flow features using unstable eigenmodes at each unstable wavenumber (left column) and with their conjugate stable eigenmodes added (right column). Simply adding one additional mode drastically decreases the difference between the true stream function and its reduced representation compared to what is

achieved with a reduced representation based on the unstable modes alone (such as those predicted by quasilinear models).<sup>41</sup>

Note that the stable and unstable eigenmodes of the KH linear operator, employed above, are related to one another by a space-time-reversal symmetry operation.<sup>31,42</sup> Thus, the unstable and stable eigenmodes transfer energy in opposite directions—the former from the mean flow to the fluctuations, while the latter in the reverse direction. The energy that is available to cascade to small scales, thus, depends on this competition. The magnitude of the energy transfer rates between the background shear-flow  $U_{ref}$  and the fluctuation scale  $k_x \neq 0$  by the unstable and stable eigenmodes can be derived from the MHD equations (see the [supplementary material](#)):  $Q_1(k_x) = \Gamma(k_x)|\beta_1(k_x)|^2$  and  $Q_2(k_x) = \Gamma(k_x)|\beta_2(k_x)|^2$ , where  $\Gamma(k_x)$  is the linear growth rate of the unstable mode at that wavenumber  $k_x$ .

The time traces of  $Q_1$  and  $Q_2$  for different  $Pm$  (resistivity) over a challenging two orders of magnitude are shown in Fig. 2. Summation over the KH-unstable wavenumbers,  $0 < k_x < 1$ , is used in determining  $Q_1$  and  $Q_2$ . Within each subplot, it is observed that  $Q_1$  and  $Q_2$  are nearly in equipartition in the nonlinear phase.

A stable-mode-excitation process may also be impacted by magnetic fields. To analyze such, we first observe the visco-resistive dissipation with varying field strengths in Figs. 3(a) and 3(b). The small-scale dissipation—a proxy of small-scale cascade—enhances with stronger fields, despite the fields reducing the linear growth rate of the instability, which sometimes is argued to lead to subdued turbulent fluctuations as the energy extraction rate by the unstable mode becomes lower.

To understand such enhanced dissipation rate, it may be instructive to compute the energy transfer rates between the background flow and the fluctuations due to both the unstable and stable eigenmodes. As seen in Fig. 3(c), the (time-averaged) energy injection rate by the instability,  $Q_1$ , decreases with stronger magnetic fields, as anticipated. However, the energy return rate by the stable modes,  $Q_2$ , is impacted more by the stronger fields, allowing larger energy cascade to small scales ( $\propto Q_1 - Q_2$ ) that manifests as enhanced dissipation rate at such scales.<sup>43</sup> Thus, a stronger magnetic field, until it nearly stabilizes the system, allows more net energy extraction from the free-energy source in the nonlinear state. This questions models that assume the linear growth rate of an instability as a surrogate for the cascade rate or a proxy for nonlinear time, see, e.g., Refs. 44–47. Predictions based upon conventional wisdom of instability-saturation are, thus, challenged.

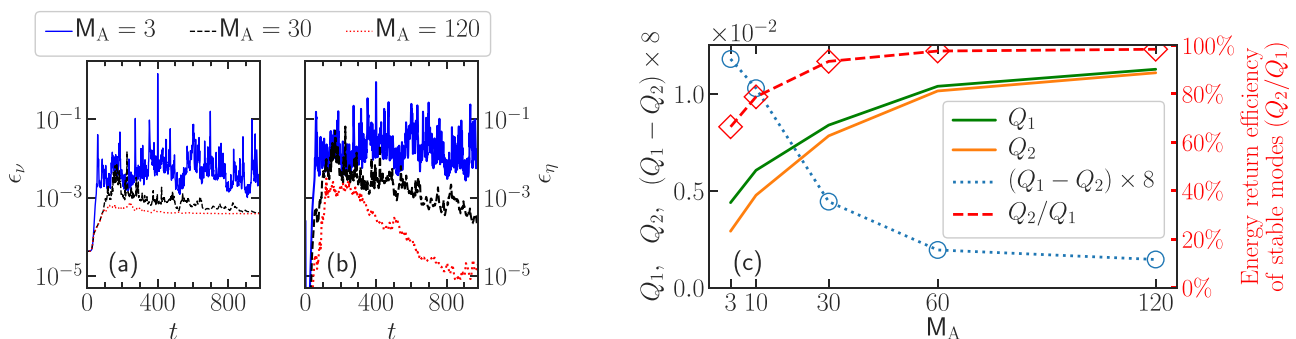


**FIG. 3.** Time traces of (a) viscous dissipation rates,  $\epsilon_v$ , and (b) resistive dissipation rates,  $\epsilon_\eta$ , for different strengths of magnetic fields. Stronger fields enhance both. (c) Impact of magnetic fields on the (time-averaged) energy transfer rates between the background profile ( $k_x = 0$ ) and the large-scale fluctuations ( $k_x = 0.2\text{--}0.8$ ) by the unstable eigenmodes  $Q_1$  and by the stable eigenmodes  $Q_2$ . Note that the magnetic fields impact  $Q_2$  more than  $Q_1$ , but  $Q_2/Q_1$  is still  $\geq 60\%$  even for the strongest field.

The ratio  $Q_2/Q_1$  of the stable-eigenmode efficiency to the unstable-eigenmode efficiency in transferring energy between the fluctuations and the background flow is more than 60% even for the strongest magnetic fields in Fig. 3(c), see the red dashed line. Such a strong Lorentz back-reaction is most potent in disrupting the vortex<sup>48</sup> and creating more small scales, leading to more reduced  $Q_2$  than the corresponding reduction in  $Q_1$ .

We now show visualizations of a highly effective role of stable modes in structuring the magnetic fields. After carrying out an initial-value simulation up to a time when the dynamics are nonlinear and turbulent, we perform two distinct simulation continuations—one unchanged with the stable modes untouched and another with the stable modes removed. For the latter, we set only the large-scale ( $0 < |k_x| < 1$ ) stable-eigenmode amplitudes to zero at the instant when the simulation is restarted. The differences immediately afterward are significant: Removing stable eigenmodes rapidly enhances the dissipation rates, see Figs. 4(a) and 4(b) (Multimedia view). To understand this increase in the dissipation, we plot the squared current density  $|\nabla^2\psi|^2$  at small scales ( $|k_x| > 1$ ) in Figs. 4(c)–4(f). Observe in Figs. 4(d) and 4(e) that the magnetic fields get rapidly distorted by the unstable modes of the flow, creating spirals as the counter-straining motion of the stable modes is removed. Note that the (un)stable modes have the largest strain around  $(x, z) \approx (10, 0)$  for the shown time, as can also be seen in the figure in the supplementary material. The stable modes here are deleted only at the instant when the simulation is paused; they are quickly nonlinearly driven back. In another simulation where the stable modes are untouched (retained), the spirals do not appear, however, and the time evolution immediately afterward remains almost identical to the initial stage [cf. Figs. 4(f) and 4(c)]. This exercise of instantaneous deletion of stable modes exposes

the true nonlinear impact of the stable modes on magnetic field evolution, which remained hidden in Fig. 1(a).

This numerical experiment illustrates that the energy injected by the unstable modes into the large-scale fluctuations ( $|k_x| < 1$ ) via mean-fluctuation interactions, *in the absence of stable modes*, cascades in its entirety to smaller scales nonlinearly where it dissipates visco-resistively. This is a statement of the classical small-scale cascade by the advective nonlinearity,  $(\mathbf{v} \cdot \nabla)\psi$ , as commonly understood. When  $\mathbf{v}$  is composed of comparable unstable and stable mode-amplitudes, though, the cascade is weakened by a factor of up to ten [Figs. 2, 3(c), and 4(b)]. Such a finding informs and can be used to improve reduced models of geo- and astrophysical instability-driven turbulence,<sup>44,50</sup> where all the energy injected by the instability is assumed to pass through an inertial cascade, e.g., Refs. 44–47.

It may be noted that, although 2D and 3D turbulence have different conserved quantities and corresponding cascade processes, the stable modes of this study are the conjugate roots of the KH-instability, which exist in both 2D and 3D.<sup>39</sup> Our preliminary studies of 3D turbulence have indeed shown that virtually identical stable mode excitation and its impact in turbulence occur in 3D as well. Details of such an investigation will be left for a future publication.<sup>49</sup>

This Letter demonstrates, for the first time, that stable modes via their counteracting straining motion of the flow, sequester magnetic energy at large scales despite the conventional association of shear-flow with intensification and generation of small scales in MHD turbulence. Our analyses show that the stable modes greatly weaken the magnetic energy cascade to small scales and, hence, can thwart the magnetic-energy accumulation at sub-viscous scales in the high-magnetic-Prandtl-number regime, typically encountered in diffuse astrophysical plasmas, thus possibly allowing operation of a dynamo

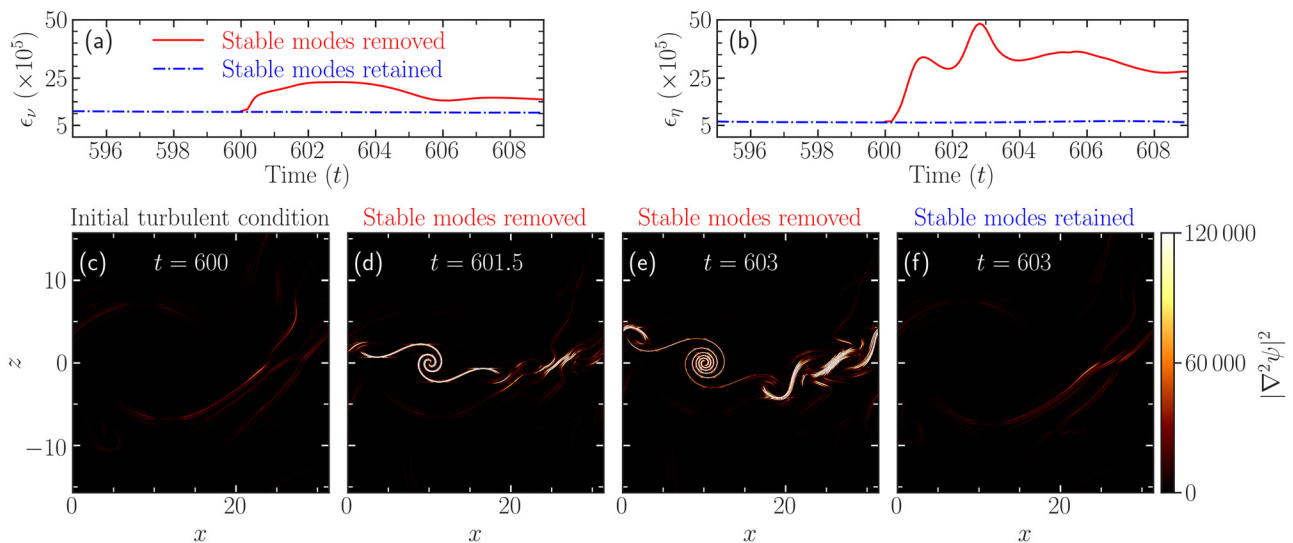


**FIG. 4.** (a) Enhancement of the viscous dissipation rate, after removing the large-scale stable eigenmodes at an instant of time  $t = 600$  in a simulation with  $M_A = 120$ . (b) Similar enhancement of the resistive dissipation. (c) The state when the simulation is paused. Shown is the squared current density at smaller scales,  $|k_x| > 1$ , focusing on the region near the shear layer,  $-5\pi \leq z \leq 5\pi$ . At this instant, the large-scale stable modes belonging to  $|k_x| < 1$  are deleted to observe their influence on the small-scale magnetic cascade. (d) and (e) Subsequent evolution of the small-scale current density when large-scale stable eigenmodes are removed at  $t = 600$ . The characteristic enfolding of magnetic fields by the eddies of unstable modes is evident, which generates small-scale magnetic features. (f) Small-scale current density in another simulation where stable eigenmodes are kept intact. The rapid straining of magnetic fields mentioned just before does not occur. For this simulation, the state at  $t = 601.5$  (not shown) is almost identical to that at  $t = 603$ . Multimedia view: <https://doi.org/10.1063/5.0096886.1>

with magnetic fields concentrated at large scales, in accord with astrophysical observations.<sup>6,10</sup> This work opens a new direction toward such studies.

See the [supplementary material](#) for the details of (I) simulation set-up, (II) modal energy evolution equation, (III) energy transfer rates between the background flow and the fluctuations, and (IV) residuals in low-order representation of the turbulent flow in [Fig. 1\(b\)](#). A simulation movie supplements [Fig. 4](#) of this Letter.

The authors thank K. Burns and Dedalus developers for assistance. The authors also thank N. Hurst for offering helpful discussions and a careful reading of the manuscript. This material is based upon the work funded by the U.S. Department of Energy (No. DE-SC0022257) through the National Science Foundation (NSF)/DOE Partnership in Basic Plasma Science and Engineering. We also gratefully acknowledge the support by the U.S. DOE under Award No. DE-FG02-04ER54742 and by the U.S. NSF under Grant Nos. AST-1814327 and AST-1908338. All simulations reported herein were performed using the supercomputing resources provided by the Extreme Science and Engineering Discovery Environment via the Allocation No. TG-PHY130027.

## AUTHOR DECLARATIONS

### Conflict of Interest

The authors have no conflicts to disclose.

### Author Contributions

**B. Tripathi:** Conceptualization (equal); Data curation (lead); Formal analysis (lead); Investigation (lead); Methodology (equal); Visualization (lead); Writing – original draft (lead); Writing – review and editing (equal). **A. E. Fraser:** Conceptualization (equal); Formal analysis (equal); Investigation (equal); Methodology (equal); Software (equal); Validation (equal); Writing – review and editing (equal). **P. W. Terry:** Conceptualization (equal); Formal analysis (equal); Funding acquisition (lead); Investigation (equal); Methodology (equal); Resources (equal); Supervision (lead); Validation (equal); Writing – review and editing (equal). **E. G. Zweibel:** Conceptualization (equal); Formal analysis (equal); Funding acquisition (lead); Investigation (equal); Methodology (equal); Resources (equal); Supervision (lead); Validation (equal); Writing – review and editing (equal). **M. J. Pueschel:** Conceptualization (equal); Formal analysis (equal); Investigation (equal); Methodology (equal); Resources (equal); Supervision (equal); Validation (equal); Writing – review and editing (equal).

### DATA AVAILABILITY

The data that support the findings of this study are available from the corresponding author upon reasonable request.

### REFERENCES

- <sup>1</sup>P. L. Johnson, “Energy transfer from large to small scales in turbulence by multiscale nonlinear strain and vorticity interactions,” *Phys. Rev. Lett.* **124**, 104501 (2020).
- <sup>2</sup>G. K. Batchelor, “On the spontaneous magnetic field in a conducting liquid in turbulent motion,” *Proc. R. Soc. London, Ser. A* **201**, 405 (1950).
- <sup>3</sup>G. K. Batchelor and I. Proudman, “The effects of rapid distortion of a fluid in turbulent motion,” *Q. J. Mech. Appl. Math.* **7**, 83 (1954).
- <sup>4</sup>A. A. Townsend, *The Structure of Turbulent Shear Flow*, 2nd ed. (Cambridge University Press, Cambridge, 1976).
- <sup>5</sup>J. Maron, S. Cowley, and J. McWilliams, “The nonlinear magnetic cascade,” *Astrophys. J.* **603**, 569 (2004).
- <sup>6</sup>A. A. Schekochihin, J. L. Maron, S. C. Cowley, and J. C. McWilliams, “The small-scale structure of magnetohydrodynamic turbulence with large magnetic Prandtl numbers,” *Astrophys. J.* **576**, 806 (2002).
- <sup>7</sup>A. Neronov and I. Vovk, “Evidence for strong extragalactic magnetic fields from Fermi observations of TeV blazars,” *Science* **328**, 73 (2010).
- <sup>8</sup>R. M. Kulsrud, “A critical review of galactic dynamos,” *Annu. Rev. Astron. Astrophys.* **37**, 37–64 (1999).
- <sup>9</sup>A. Brandenburg and K. Subramanian, “Astrophysical magnetic fields and nonlinear dynamo theory,” *Phys. Rep.* **417**, 1–209 (2005).
- <sup>10</sup>S. M. Tobias and F. Cattaneo, “Shear-driven dynamo waves at high magnetic Reynolds number,” *Nature* **497**, 463 (2013).
- <sup>11</sup>J. Squire and A. Bhattacharjee, “Generation of large-scale magnetic fields by small-scale dynamo in shear flows,” *Phys. Rev. Lett.* **115**, 175003 (2015).
- <sup>12</sup>D. R. Hatch, P. W. Terry, F. Jenko, F. Merz, and W. M. Nevins, “Saturation of gyrokinetic turbulence through damped eigenmodes,” *Phys. Rev. Lett.* **106**, 115003 (2011).
- <sup>13</sup>A. E. Fraser, P. W. Terry, E. G. Zweibel, and M. J. Pueschel, “Coupling of damped and growing modes in unstable shear flow,” *Phys. Plasmas* **24**, 062304 (2017).
- <sup>14</sup>A. E. Fraser, P. W. Terry, E. G. Zweibel, M. J. Pueschel, and J. M. Schroeder, “The impact of magnetic fields on momentum transport and saturation of shear-flow instability by stable modes,” *Phys. Plasmas* **28**, 022309 (2021).
- <sup>15</sup>P. W. Terry, B. J. Faber, C. C. Hegna, V. V. Mirnov, M. J. Pueschel, and G. G. Whelan, “Saturation scalings of toroidal ion temperature gradient turbulence,” *Phys. Plasmas* **25**, 012308 (2018).
- <sup>16</sup>G. G. Whelan, M. J. Pueschel, and P. W. Terry, “Nonlinear electromagnetic stabilization of plasma microturbulence,” *Phys. Rev. Lett.* **120**, 175002 (2018).
- <sup>17</sup>A. E. Fraser, M. J. Pueschel, P. W. Terry, and E. G. Zweibel, “Role of stable modes in driven shear-flow turbulence,” *Phys. Plasmas* **25**, 122303 (2018).
- <sup>18</sup>M. J. Pueschel, B. J. Faber, J. Citrin, C. C. Hegna, P. W. Terry, and D. R. Hatch, “Stellarator turbulence: Subdominant eigenmodes and quasilinear modeling,” *Phys. Rev. Lett.* **116**, 085001 (2016).
- <sup>19</sup>K. D. Makwana, P. W. Terry, M. J. Pueschel, and D. R. Hatch, “Subdominant modes in zonal-flow-regulated turbulence,” *Phys. Rev. Lett.* **112**, 095002 (2014).
- <sup>20</sup>D. R. Hatch, F. Jenko, A. B. Navarro, and V. Bratanov, “Transition between saturation regimes of gyrokinetic turbulence,” *Phys. Rev. Lett.* **111**, 175001 (2013).
- <sup>21</sup>K. D. Makwana, P. W. Terry, and J.-H. Kim, “Role of stable modes in zonal flow regulated turbulence,” *Phys. Plasmas* **19**, 062310 (2012).
- <sup>22</sup>K. D. Makwana, P. W. Terry, J.-H. Kim, and D. R. Hatch, “Damped eigenmode saturation in plasma fluid turbulence,” *Phys. Plasmas* **18**, 012302 (2011).
- <sup>23</sup>P. W. Terry, D. A. Baver, and S. Gupta, “Role of stable eigenmodes in saturated local plasma turbulence,” *Phys. Plasmas* **13**, 022307 (2006).
- <sup>24</sup>D. Biskamp, *Magnetohydrodynamic Turbulence* (Cambridge University Press, 2003).
- <sup>25</sup>M. J. Pueschel, D. Told, P. W. Terry, F. Jenko, E. G. Zweibel, V. Zhankin, and H. Lesch, “Magnetic reconnection turbulence in strong guide fields: Basic properties and application to coronal heating,” *Astrophys. J., Suppl. Ser.* **213**, 30 (2014).
- <sup>26</sup>J. B. Marston, E. Conover, and T. Schneider, “Statistics of an unstable barotropic jet from a cumulant expansion,” *J. Atmos. Sci.* **65**, 1955 (2008).
- <sup>27</sup>K. M. Smith, C. P. Caulfield, and J. R. Taylor, “Turbulence in forced stratified shear flows,” *J. Fluid Mech.* **910**, A42 (2021).
- <sup>28</sup>A. Allawala, S. M. Tobias, and J. B. Marston, “Dimensional reduction of direct statistical simulation,” *J. Fluid Mech.* **898**, A21 (2020).
- <sup>29</sup>K. J. Burns, G. M. Vasil, J. S. Oishi, D. Lecoanet, and B. P. Brown, “Dedalus: A flexible framework for numerical simulations with spectral methods,” *Phys. Rev. Res.* **2**, 023068 (2020).
- <sup>30</sup>This is because the dissipationless linear operator respects the parity-time-reversal symmetry operation, and hence, its eigenmodes can be proven to form a complete basis, see Ref. 31.
- <sup>31</sup>C. M. Bender, *PT Symmetry: In Quantum and Classical Physics* (World Scientific, 2019).

- <sup>32</sup>B. Tripathi, A. E. Fraser, P. W. Terry, E. G. Zweibel, and M. J. Pueschel, "Near-cancellation of up- and down-gradient momentum transport in forced magnetized shear-flow turbulence," *Phys. Plasmas* (submitted) (2022).
- <sup>33</sup>Energy norm is used to normalize the eigenmodes.
- <sup>34</sup>Some similarities can be identified between the state-space reconstruction via this method and other approaches of modeling turbulence, e.g., exact coherent structures<sup>35</sup> and proper orthogonal decomposition.<sup>36</sup>
- <sup>35</sup>B. Suri, J. Tithof, R. O. Grigoriev, and M. F. Schatz, "Forecasting fluid flows using the geometry of turbulence," *Phys. Rev. Lett.* **118**, 114501 (2017).
- <sup>36</sup>K. Taira, S. L. Brunton, S. T. M. Dawson, C. W. Rowley, T. Colonius, B. J. McKeon, O. T. Schmidt, S. Gordeyev, V. Theofilis, and L. S. Ukeiley, "Modal analysis of fluid flows: An overview," *AIAA J.* **55**, 4013 (2017).
- <sup>37</sup>A. Ishizawa, Y. Kishimoto, and Y. Nakamura, "Multi-scale interactions between turbulence and magnetic islands and parity mixture—A review," *Plasma Phys. Controlled Fusion* **61**, 054006 (2019).
- <sup>38</sup>M. Sato and A. Ishizawa, "Nonlinear parity mixtures controlling the propagation of interchange modes," *Phys. Plasmas* **24**, 082501 (2017).
- <sup>39</sup>S. Chandrasekhar, *Hydrodynamic and Hydromagnetic Stability* (Clarendon Press, Oxford, 1961).
- <sup>40</sup>K. M. Case, "Stability of inviscid plane Couette flow," *Phys. Fluids* **3**, 143 (1960).
- <sup>41</sup>Thus, reconstructed flow includes components that strain the magnetic field efficiently. The turbulent magnetic field, in contrast, requires many eigenmodes for each wavenumber. This is consistent with the fluid-straining-induced generation of small scales of the magnetic field which, when projected onto the eigenmode space, covers a large number of marginally stable continuum eigenmodes.
- <sup>42</sup>Y. Fu and H. Qin, "The physics of spontaneous parity-time symmetry breaking in the Kelvin-Helmholtz instability," *New J. Phys.* **22**, 083040 (2020).
- <sup>43</sup>Essentially, the same conclusion has been found by recomputing  $Q_1$  and  $Q_2$  where they refer to the transfer rates between the fluctuations and the *instantaneous* mean profiles.
- <sup>44</sup>J. Fuller, A. L. Piro, and A. S. Jermyn, "Slowing the spins of stellar cores," *Mon. Not. R. Astron. Soc.* **485**, 3661 (2019).
- <sup>45</sup>M. E. Pessah, C.-K. Chan, and D. Psaltis, "The signature of the magnetorotational instability in the Reynolds and Maxwell stress tensors in accretion discs," *Mon. Not. R. Astron. Soc.* **372**, 183 (2006).
- <sup>46</sup>J. Goodman and G. Xu, "Parasitic instabilities in magnetized, differentially rotating disks," *Astrophys. J.* **432**, 213 (1994).
- <sup>47</sup>P. Garaud, "Double-diffusive convection at low Prandtl number," *Annu. Rev. Fluid Mech.* **50**, 275 (2018).
- <sup>48</sup>J. Mak, S. D. Griffiths, and D. W. Hughes, "Vortex disruption by magnetohydrodynamic feedback," *Phys. Rev. Fluids* **2**, 113701 (2017).
- <sup>49</sup>B. Tripathi, A. E. Fraser, P. W. Terry, E. G. Zweibel, M. J. Pueschel, and E. H. Anders, "Testing quasilinear theories in shear-flow turbulence," (unpublished).
- <sup>50</sup>A. VanDine, H. T. Pham, and S. Sarkar, "Turbulent shear layers in a uniformly stratified background: DNS at high Reynolds number," *J. Fluid Mech.* **916**, A42 (2021).